Cellular and Molecular Life Sciences (2022) 79:457
https://doi.org/10.1007/s00018-022-04492-y

ORIGINAL ARTICLE

$A\beta_{1-42}$ peptides blunt the adenosine A_{2A} receptor-mediated control of the interplay between P_2X_7 and P_2Y_1 receptors mediated calcium responses in astrocytes

Liliana Dias[1,3] · Daniela Madeira[1,3] · Rafael Dias[1] · Ângelo R. Tomé[1,2] · Rodrigo A. Cunha[1,3] · Paula Agostinho[1,3]

Received: 12 April 2022 / Revised: 22 June 2022 / Accepted: 15 July 2022 / Published online: 30 July 2022

Abstract

The contribution of astrocytes to Alzheimer's disease (AD) is still ill defined. AD involves an abnormal accumulation of amyloid-β peptides (Aβ) and increased production of danger signals such as ATP. ATP can direct or indirectly, through its metabolism into adenosine, trigger adaptive astrocytic responses resulting from intracellular Ca^{2+} oscillations. AD also triggers an upregulation of astrocytic adenosine A_{2A} receptors ($A_{2A}R$), which blockade prevents memory dysfunction in AD. We now investigated how Aβ peptides affect ATP-mediated Ca^{2+} responses in astrocytes measured by fluorescence live-cell imaging and whether $A_{2A}R$ control astrocytic Ca^{2+} responses mediated by ATP receptors, mainly P_2X_7R and P_2Y_1R. In primary cultures of rat astrocytes exposed to $A\beta_{1-42}$, ATP-evoked Ca^{2+} responses had a lower amplitude but a longer duration than in control astrocytes and involved P_2X_7R and P_2Y_1R, the former potentiating the later. Moreover, $A\beta_{1-42}$ exposure increased protein levels of P_2Y_1R in astrocytes. $A_{2A}R$ antagonism with SCH58261 controlled in a protein kinase A-dependent manner both P_2X_7R- and P_2Y_1R-mediated Ca^{2+} responses in astrocytes. The interplay between these purinoceptors in astrocytes was blunted upon exposure to $A\beta_{1-42}$. These findings uncover the ability of $A_{2A}R$ to regulate the inter-twinned P_2X_7R- and P_2Y_1R-mediated Ca^{2+} dynamics in astrocytes, which is disrupted in conditions of early AD.

Keywords Astrocyte · Ca^{2+} dynamics · Alzheimer's disease · P2 receptors · Adenosine A_{2A} receptors

Abbreviations

Aβ	Amyloid-beta peptides
AD	Alzheimer's disease
$A_{2A}R$	Adenosine A_{2A} receptors
$[Ca^{2+}]_i$	Intracellular Ca^{2+} concentration
$\Delta[Ca^{2+}]_i$	Changes in intracellular Ca^{2+} concentration induced by a stimulus
ER	Endoplasmic reticulum
IP_3R	Inositol 1,3,5-trisphosphate receptors
P_2X_7R	P_2X_7 receptors
P_2Y_1R	P_2Y_1 receptors
PBS	Phosphate-buffered saline

✉ Paula Agostinho
pagostinho@fmed.uc.pt

1 CNC-Center for Neuroscience and Cell Biology, University of Coimbra, Rua Larga, Polo I FMUC, 1st Floor, 3004-504 Coimbra, Portugal

2 Department of Life Sciences, Faculty of Sciences and Technology, University of Coimbra, Coimbra, Portugal

3 Faculty of Medicine, University of Coimbra, Rua Larga, Polo I FMUC, 1st Floor, 3004-504 Coimbra, Portugal

Introduction

Astrocytes are characteristic glial cells with several processes that tile the entire CNS [1, 2]. Besides their essential supportive role, astroglia cells have a large spectrum of functions in brain, including regulation of blood flow, metabolic support to neurons, ionic homeostasis, clearance of neurotransmitters, regulation of extracellular space volume and the modulation of synaptic activity [3–6]. Although astrocytes are considered electrically non-excitable cells because they do not fire action potentials, their responsiveness entails ionic signaling typified by the generation of spatio-temporal Ca^{2+} oscillations [7–9]. These astrocytic Ca^{2+} oscillations consist mainly in a transient increase in intracellular Ca^{2+} concentration, which can propagate across and between astrocytes, to drive their adaption to information flowing in neuronal circuits [10–13]. In fact, astrocytic Ca^{2+} signaling mediates different astrocytic

adaptive functions, namely Ca^{2+}-dependent exocytotic gliotransmitters release, excitability and activation of transduction signaling pathways, which in turn impact on neuronal function [3, 8, 14, 15].

Astrocytes have several ionotropic and metabotropic receptors able to trigger Ca^{2+} entry or Ca^{2+} release from inositol 1,4,5-trisphosphate (IP_3)-sensitive intracellular Ca^{2+} stores, mainly from the endoplasmic reticulum (ER) [10, 16–19]. One such group of receptors are purinergic receptors, encompassing P_1 receptors, a family of protein G-coupled metabotropic adenosine (A_1, A_{2A}, A_{2B}, A_3) receptors, and P_2 receptors for ATP that are sub-divided into $P_2X_{(1-7)}$ channels and G protein-coupled metabotropic $P_2Y_{(1-12)}$ receptors. These receptors are part of signaling pathways involved in astrocyte–astrocyte and neuron–astrocyte communication; they sense activity and danger signals conveyed by purines, and regulate a wide range of physiological and pathological processes [20, 21]. Accordingly, purine receptors may contribute to the pathogenesis of Alzheimer's disease (AD) [22, 23], a neurodegenerative disorder considered to be caused by amyloid-β peptides (Aβ) accumulation.

Our group demonstrated that purinergic receptors, in particular adenosine A_{2A} receptors ($A_{2A}R$) overfunction is sufficient to disrupt memory performance [24, 25]; $A_{2A}R$ are also strictly necessary to trigger synaptic and memory deficits in the early AD phases, which are abrogated by $A_{2A}R$ blockade [26, 27]. $A_{2A}R$ are also present in astrocytes, being upregulated in both AD patients and mouse models [28, 29], as well as in cultured astrocytes exposed to synthetic $A\beta_{1-42}$ [28, 30], which is widely used to mimic AD pathology. Moreover, astrocytic $A_{2A}R$ control the levels of GLT-1 glutamate transporters and regulate the Na^+/K^+ activity and their blockade alleviates the impairment of glutamate uptake triggered by $A\beta_{1-42}$ in cultured astrocytes [28, 31, 32]. This complements the increasing evidences indicating that astrocytes respond to Aβ peptides triggering altered signaling pathways, such as abnormal increases in intracellular Ca^{2+} levels [13, 33]. Astrocytic Ca^{2+} hyperactivity contributes to altered brain cortical function such as memory, and progressively declines in AD [34, 35]. The appearance of this hyperactive Ca^{2+} dynamics is claimed to be associated with abnormal purinergic signaling in reactive astrocytes, which have an altered morphology and function in the initial the phases of AD [21, 23, 35]. However, the ability of $A\beta_{1-42}$ to modify the purinergic control of astrocytic Ca^{2+} dynamics remains untested. The present study aims to fill this gap of knowledge by studying how $A_{2A}R$ control astrocytic Ca^{2+} dynamics evoked by ATP, a ubiquitous signaling molecule that is rapidly metabolized into adenosine, and how the exposure to $A\beta_{1-42}$ influences the purinergic control of astrocytic Ca^{2+} dynamics.

Materials and methods

Primary astrocyte cultures from Wistar rats

The experiments were performed using primary cultures of astrocytes from the cerebral cortex of post-natal Wistar rat pups with 1–3 days of age. Rats were born at our animal facilities, and their use was approved by the Institution's Ethical Committee (ORBEA128_2015/04122015) and certified by *Direção Geral de Alimentação e Veterinaria* (DGAV; 0421/000/000/2016 Ref. 014420), and conducted in agreement with standard procedures to reduce animal suffering and number, in accordance with European legislation on animal welfare.

Astrocytic cultures were prepared according with a protocol previously described by us [30], with some modifications. In brief, after Wistar pups killing (6–8 animals per preparation), the brain cortices were dissected in a cold plate (4 ºC) and mechanically dissociated using a scalpel. This tissue was placed in 5 mL of pre-warmed TrypLE reagent (Gibco), an enzyme solution used for cell dissociation, supplemented with DNAse I (10 mg/mL in 10 mM NaCl, Sigma Aldrich). This enzymatic digestion was stopped by adding a high glucose (4.5 g/L) Dulbecco's Modified Eagle Medium (DMEM), supplemented with 10% fetal bovine serum (FBS) and 10 mL/L penicillin–streptomycin, pH 7.4. Cell suspension was centrifuged at $115 \times g$ for 2 min and the pellet was resuspended in culture medium. After determining the cell number per mL of solution, the dissociated cells were placed in T75 flasks pre-coated with poly-D-lysine (0.1 mg/mL in borate buffer, pH 8.2), at a density of 1×10^5 cells/cm^3. The cells were maintained at 37 ºC in a humidified 5% CO_2 incubator for 14–15 days until reach confluency. During this period, the cultures were shaken (speed 200 rpm) every 2–3 days for 4 h at 37 ºC, to detach microglia from the astrocyte monolayer, followed by replacement of the culture medium to remove microglia in suspension. Afterwards, astrocytes were detached from bottom flasks using a mild trypsinization protocol [30], in which cells were washed with PBS (135 mM NaCl, 2.7 mM KCl, 4.3 mM Na_2HPO_4, 1.47 mM KH_2PO_4) with 1 mM EDTA and further detached using 0.05% trypsin (Sigma Aldrich) in PBS solution. Cell suspension was centrifuged at $180 \times g$ for 5 min and astrocytes were plated in 35 mm high glass bottom imaging dishes (Ibidi, #81156) or 48-well multiplate at a density of 1.14×10^4 or 26×10^4 cells/cm^2, respectively, for Ca^{2+} experiments; or at a density of 26×10^4 cells/cm^2 in 12-well multiplate for Western-blot assays. Astrocytes remained in culture for 2 days, before performing the experiments.

The percentage of astrocytes and microglia in our cultures were assessed by immunolabelling the cell cultures with antibodies that recognize the skeleton astrocytic

protein, glial fibrillary acidic protein (GFAP) and the microglia marker protein CD11b. As can be seen in Fig. S1, our cultures were enriched in astrocytes, corresponding to about 95% of the cells, and had only a residual amount of microglia cells (< 5%).

Astrocytes exposure to $A\beta_{1-42}$ peptides

To mimic AD-like conditions, cultured astrocytes were incubated with the synthetic peptide $A\beta_{1-42}$ (Bachem, #4014447), at a final concentration of 1 µM. This peptide was dissolved in 0.1% NH_4OH solution at a stock concentration of 221.5 µM and stored at − 20 °C until used. $A\beta_{1-42}$ solution contained mainly soluble monomers and oligomers, as previously reported by us [26, 28] and others [25]. For Ca^{2+} measurement assays, the peptide was added to culture medium for 1 h prior to Ca^{2+} probe incubation, whereas in studies assessing protein levels, the incubation time of $A\beta_{1-42}$ with astrocytes was 24 h.

Intracellular [Ca^{2+}] measurements

Cultured astrocytes were incubated for 45 min with Fluo-4-AM (4 µM; Life Technologies) dissolved in recording buffer (132 mM NaCl, 4 mM KCl, 1.4 mM $MgCl_2$, 6 mM glucose, 10 mM HEPES, 1.8 mM $CaCl_2$; pH 7.4) with 0.05% bovine serum albumin to facilitate probe entry into cells. Then, the cells were washed and left in recording buffer for 15 min to allow complete Fluo-4 AM de-esterification. In some experimental conditions, the following modifiers of Ca^{2+} dynamics were added to recording buffer during the de-esterification period and kept until the end of experiment: the selective P_{2X7} receptor antagonist 2-(phenylthio)-*N*-[[tetrahydro-4-(4-phenyl-1-piperazinyl)-2*H*-pyran-4-yl] methyl-3-pyridinecarboxamide (JNJ47965567, 1 µM, Tocris), the selective P_{2Y1} receptor antagonist 2′-deoxy-N^6-methyladenosine 3′,5′-bisphosphate tetrasodium salt (MRS2179, 30 µM, Tocris), the selective A_{2A} receptor antagonist 2-(2-furanyl)-7-(2-phenylethyl)-7*H*-pyrazolo[4,3-e][1,2,4]triazolo[1,5-c]pyrimidin-5-amine (SCH58261, 50 nM, Tocris) or the selective protein kinase A (PKA) inhibitor *N*-[2-[[3-(4-bromophenyl)-2-propenyl]amino] ethyl]-5-isoquinolinesulfonamide (H-89, 10 µM, Tocris).

After de-esterification, Ca^{2+} fluorescence was recorded using a VICTOR^3 multiplate reader (Perkin Helmer, RRID: SCR_019232) with Wallac 1420 software. The baseline fluorescence of the Ca^{2+} probe was recorded during 5 min with a delay of 5 s between acquisitions. Ca^{2+} transients were evoked by different stimuli, either the purinergic agonist adenosine 5′-triphosphate (ATP, 100 µM, Sigma Aldrich), the selective P_{2X7} receptor agonist 2′(3′)-*O*-(4-benzoylbenzoyl)adenosine 5′-triphosphate (BzATP, 100 µM, Sigma Aldrich) or the selective P_{2Y1} receptor agonist [[(1R,2R,3S,4R,5S)-4-[6-amino-2-(methylthio)-9H-purin-9-yl]-2,3-dihydroxybicyclo[3.1.0]hex-1-yl]methyl] diphosphoric acid (MRS2365, 10 nM, Tocris) and fluorescence was recorded for 5 min. After recording the stimulus-evoked Ca^{2+} response, cells were exposed to ionomycin (10 µM, Santa Cruz) allowing extracellular Ca^{2+} entry thus triggering the maximum fluorescence response.

The fluorescence data were background-corrected by subtracting the mean fluorescence value of astrocytes that were not incubated with Fluo-4-AM. Intracellular calcium concentration was estimated for each time point using the formula: $[Ca^{2+}] = K_d \times (F - F_{min})/(F_{max} - F)$, in which K_d is the dissociation constant of Fluo-4 (345 nM), F corresponds to the fluorescence recorded at each time point, F_{max} is the maximum fluorescence obtained by ionomycin application and F_{min} is the minimum fluorescence. The amplitude of [Ca^{2+}] transients triggered by each stimulus was obtained subtracting the mean of basal levels from the maximum value after stimulus application. Data are presented as variation in [Ca^{2+}] (Δ[Ca^{2+}]), expressed in nM.

Live-cell Ca^{2+} imaging experiments

Astrocytes were incubated for 45 min with the fluorescent Ca^{2+}-binding probe Fluo-4-AM (4 µL in DMSO, Life Technologies) in Krebs buffer (132 mM NaCl, 4 mM KCl, 1.4 mM MgCl, 6 mM glucose, 10 mM HEPES, 1.8 mM $CaCl_2$; pH 7.4) with 0.05% bovine serum albumin. After incubation, cells were washed and kept in recording buffer for 15 min to ensure complete probe de-esterification.

After de-esterification, Ibidi dishes (cat#81156) were mounted in the stage of a Spinning Disk inverted microscope (Axio Observer Z1, Zeiss), equipped with a chamber for temperature control (37 ºC). Fluo-4 loaded cells were excited with a solid-state laser at 488 nm and the emission fluorescence was passed through a band-pass (BP) filter and measured at 525/50 nm. All experiments were recorded with an EM-CCD digital camera (Electron Multiplying-Charged Coupled Device, Photometrics Evolve™ 512 Delta) and data acquisition was controlled by Zen software. To minimize fluorescence bleaching, the excitation light and sampling frequency were kept as low as possible.

Astrocytic Ca^{2+} responses were triggered with ATP (100 µM, Sigma Aldrich) in the absence or presence of the different purinergic receptor ligands listed above and fluorescence was measured in intervals of 500 ms.

Data analysis of live-cell Ca^{2+} imaging experiments

Data from live-cell Ca^{2+} fluorescent measurements were imported to Image J to manually define regions of interest (ROIs), drawn around each cell body. Ca^{2+} signals were estimated in these ROIs as F/F_B, where F is the fluorescence

intensity for each time point and F_B is the baseline fluorescence, before stimulus application, both background corrected. To define background contribution, ROIs were drawn in regions lacking dye-filled structures and this mean background fluorescence was subtracted at each time point. Graphical representations of Ca^{2+} variations over time allowed to calculate: (i) amplitude and (ii) duration of ATP-evoked response. Amplitude of the response was calculated by subtracting the mean intensities before ATP application to the maximum value of the fluorescence response of the Ca^{2+} indicator; duration corresponds to the difference between the end of the response and the time of ATP application; magnitude was calculated by determining the area under the curve of the evoked Ca^{2+} response. On average, 40 cells were analyzed per experiment and non-responsive astrocytes were excluded from analysis.

Western blot experiments

Astrocytes were treated with SCH58261 (50 nM, Tocris) 30 min prior to challenge with $A\beta_{1-42}$ peptides (1 µM) for 24 h. Similarly P2 receptors antagonists MRS2179 (30 µM, Tocris), JNJ47965567 (1 µM, Tocris), pyridoxalphosphate-6-azophenyl-2′,4′-disulfonic acid tetrasodium salt (PPADS, 10 µM, Abcam) and reactive blue 2 (RB-2, 2 µM, Sigma) were incubated for 24 h before analysis. After these incubations, the cells were washed twice with PBS and gently scraped with ice-cold lysis buffer RIPA [50 mM Tris, 150 mM NaCl, 1.0% IGEPAL (NP-40), 0.5% sodium deoxycholate, 1 mM EDTA and 0.1% SDS, pH 8.0 supplemented with 1 mM DTT, 1 mM PMSF and 0.001% CLAP]. Then, the protein concentration of samples was quantified using the bicinchoninic acid method (BCA, Thermo Scientific). The samples were denaturated by heating at 70 ºC for 20 min, following the addition of 6 × concentrated sample buffer (500 mM Tris, 600 mM dithiothreitol, 10.3% sodium dodecyl sulfate, 30% glycerol and 0.012% bromophenol). Samples containing 10 µg or 20 µg of protein were used to assess P_2X_7R and P_2Y_1R levels, respectively. The subsequent Western blot assay was performed as previously described [see 26, 28, 30]. Briefly, electrophoresis was performed by loading the 5–10 µL of samples into 10% polyacrylamide SDS-PAGE gels for protein separation. Proteins were then electro-transferred to nitrocellulose membranes (GE Healthcare). Nonspecific binding was blocked with 5% non-fat dry milk in Tris-buffered saline (TBS, 20 mM Tris, 137 mM NaCl, pH 7.6) containing 0.1% Tween 20 for 1 h at room temperature, under agitation [30]. The membranes were further incubated overnight at 4 ºC with the primary antibodies: rabbit anti-$P_{2X7}R$ (1:200, Santa Cruz Biotechnology, RRID: AB_2158373) or rabbit anti-$P_{2Y1}R$ (1:1000, Cell Signaling Technology). After rinsing with TBS-T, the membranes were incubated with the appropriate peroxidase-conjugated goat anti-rabbit IgG secondary antibody (1:5000, Thermo Fisher Scientific, RRID: AB_228338) for 2 h at room temperature. Membranes were revealed with enhanced chemiluminescence substrate (GE Healthcare) and visualized using an imaging system (Chemidoc, RRID: SCR_021693). The membranes were reprobed for β-actin (1:20,000, Sigma Aldrich, RRID: AB_47674) and peroxidase-conjugated goat anti-mouse IgG secondary antibody (1:5000, Thermo Fisher Scientific, RRID: AB_228302) to control for protein loading. The densitometric analysis of protein bands was performed using Image Lab Software with the version 5.2.1 (Bio-Rad, RRID: SCR_014210).

Immunocytochemistry

Astrocytes seeded in poly-D-lysine-coated coverslips were fixed in 4% paraformaldehyde in PBS for 15 min. Then, the cells were permeabilized with 0.2% Triton X-100 solution in PBS for 10 min and non-specific binding of antibodies was blocked with 3% bovine serum albumin and 5% horse serum in PBS for 1 h. Subsequently, astrocytes were incubated with the primary antibodies, namely rabbit anti-GFAP (1:100, Millipore, RRID:AB_2109645) and mouse anti-CD11b (1:200; Serotec, RRID:AB_321302) for 2 h at room temperature. After three washes with 3% bovine serum albumin in PBS, cells were incubated with the secondary antibodies donkey anti-mouse 488 (1:500; Thermo Fisher Scientific, RRID:AB_141607) and donkey anti-rabbit 594 (1:500; Thermo Fisher Scientific, RRID: AB_141637) for 1 h at room temperature, protected from light. The immunolabeled cells were then stained with nuclei dye DAPI in PBS (0.1%, Invitrogen) for 3 min. Finally, the coverslips were mounted in fluorescent mounting medium (Dako) and visualized in an epifluorescence microscope (Zeiss, Axio Imager Z2 microscope, RRID:SCR_018856 with AxioVision Imaging System, RRID:SCR_002677 version 4.8). Images obtained from random fields were analyzed using the ImageJ software (RRID: SCR_003070).

Statistical data analysis

Data from live-cell Ca^{2+} imaging were expressed as increase of fluorescence in arbitrary units (a.u.) for amplitude and expressed in seconds (s) for ATP-evoked response duration. Results obtained from multiplate Ca^{2+} measurements were presented as intracellular Ca^{2+} concentration expressed in nM, whereas protein levels determined in Western blot assays were expressed as percentage relatively to control (non-treated astrocytes). All data were presented as mean ± SEM of *n* independent experiments, i.e., experiments performed using astrocytes cultures prepared in different days. Statistical analysis was carried out using Mann–Whitney non-parametric tests in live-cells experiments, whereas

the multiplate Ca^{2+} measurements were evaluated using one-way ANOVA followed by Dunnett multiple comparison post hoc test or two-way ANOVA followed by Tukey multiple comparison post hoc test, depending on the presence of one or more variables, respectively. The confidence interval was set as 95% so that the difference between means was considered significant at p values of less than 5% (0.05), 1% (0.01) and 0.1% (0.001) of significance level (α). In the analysis of protein levels, the experimental group was compared with a hypothetical value of 100 (control) using one sample t test or evaluated using two-way ANOVA followed by Tukey multiple comparison post hoc test in the presence of two variables. Data were analyzed using GraphPad Prism software, version 6.0 (RRID: SCR_00279).

Results

Effect of $A\beta_{1-42}$ exposure on astrocytic Ca^{2+} dynamics

We used primary cultures of astrocytes to evaluate intracellular Ca^{2+} oscillations triggered by ATP (100 µM) [36] in control astrocytes and in astrocytes previously exposed to $A\beta_{1-42}$ (1 µM, for 1 h), to mimic AD-like conditions. Exposure to $A\beta_{1-42}$ induced a slight non-statistically significant increase ($p > 0.05$, $n = 9–11$) in basal $[Ca^{2+}]_i$ from 175.3 ± 13.14 nM in non-treated cells (CTRL) to 198.4 ± 18.68 nM in astrocytes treated with $A\beta_{1-42}$ (Fig. 1A). Notably, ATP stimulation induced a significant lower $[Ca^{2+}]_i$ response in $A\beta_{1-42}$-treated compared with control astrocytes (CTRL: 218.90 ± 29.52 nM vs. $A\beta_{1-42}$: 130.30 ± 17.88; $p < 0.05$, $n = 7–11$, Fig. 1B). These data lead us to further investigate some parameters of Ca^{2+} dynamic response, such as their amplitude and duration [36, 37]. ATP evoked

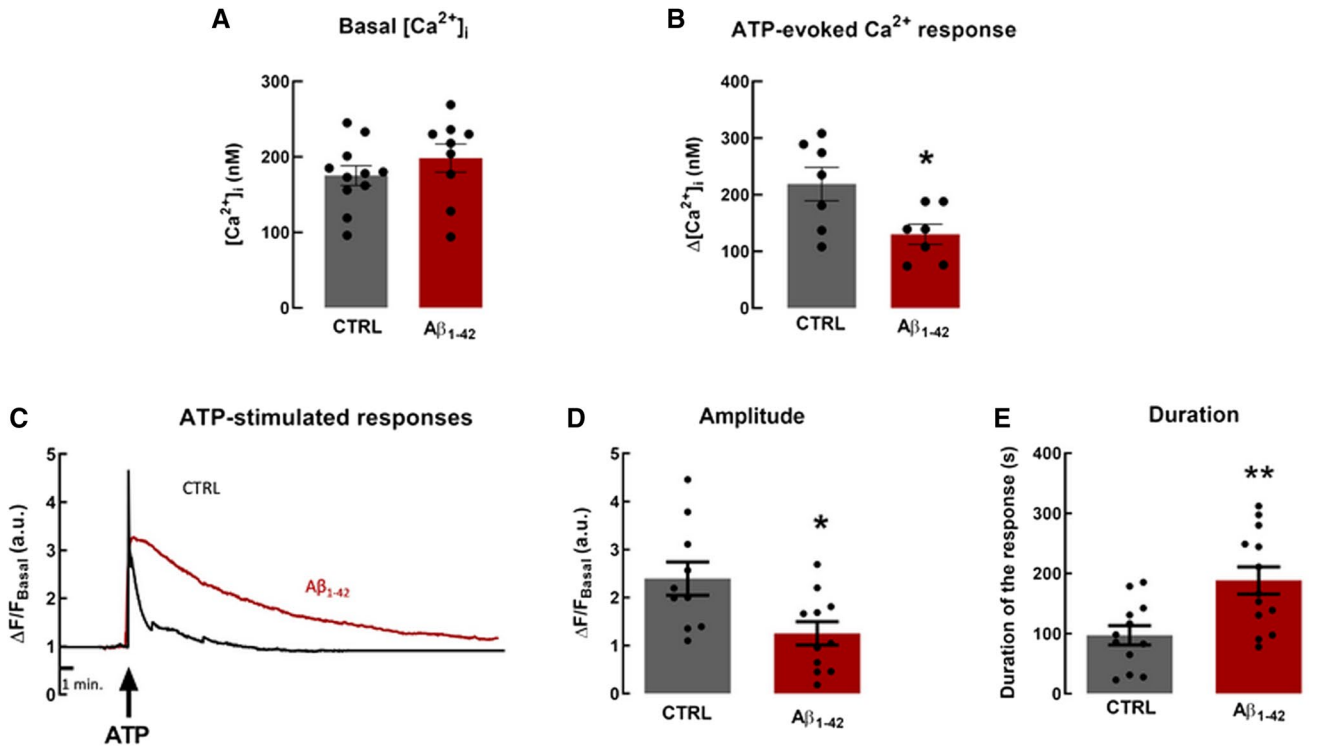

Fig. 1 $A\beta_{1-42}$ induced alterations of ATP-induced astrocytic Ca^{2+} responses but not of basal Ca^{2+} levels. Basal intracellular Ca^{2+} concentration ($[Ca^{2+}]_i$, (**A**) and increases in intracellular Ca^{2+} concentration ($\Delta[Ca^{2+}]_i$) evoked by 100 µM ATP (**B**) in cultured astrocytes not exposed (CTRL) or exposed to $A\beta_{1-42}$ (1 µM, for 1 h). $A\beta_{1-42}$ exposure did not affect basal Ca^{2+} levels, but decrease the $\Delta[Ca^{2+}]_i$ evoked by ATP. Data are mean ± SEM of 7–11 independent experiments. **C** Representative time course of single-cell fluorescence Ca^{2+} imaging in cultured astrocytes exposed to $A\beta_{1-42}$ or not exposed to it (CTRL), which were stimulated with ATP (100 µM). The fluorescence values were measured in a spinning-disk microscope and are expressed as the ratio of change in fluorescence, to quantify the amplitude (**D**), i.e., peak or increase over basal fluorescence (expressed in arbitrary units, a.u.), and the duration (**E**, expressed in seconds, s) of Ca^{2+} response evoked by ATP. Exposure to $A\beta_{1-42}$ decreased the amplitude of Ca^{2+} response but increased the duration of the Ca^{2+} response as compared to control astrocytes. Data are mean ± SEM of 10–12 independent experiments. $^*p < 0.05$, $^{**}p < 0.01$ as compared to control, Mann–Whitney test; $n = 10–13$. Each experiment represents the mean values of approximately 40 co-cultured astrocytes

a rapid transient $[Ca^{2+}]_i$ rise that decayed towards basal level in more than 95% of the astrocytes, although some cells also exhibited a response with multiple consecutive peaks. However, in astrocytes exposed to $A\beta_{1-42}$ (1 µM, for 1 h), ATP stimulation evoked a Ca^{2+} response with a reduced peak or amplitude that took longer to decay, i.e., with a longer duration, as compared with control astrocytes (Fig. 1C). Thus, the amplitude of ATP-evoked Ca^{2+} response was significantly ($p < 0.05$) reduced in $A\beta_{1-42}$-exposed astrocytes (1.22 ± 0.23 a.u., $n = 12$, 309 cells) compared with control astrocytes (2.40 ± 0.35 a.u., $n = 9$, 324 cells); this corresponds to a 49% decrease of the response amplitude by $A\beta_{1-42}$ (Fig. 1D). In contrast, the duration of Ca^{2+} responses was significantly longer ($p < 0.01$) in astrocytes exposed to $A\beta_{1-42}$ (188.30 ± 22.73 s, $n = 13$, 342 cells) lasting in average nearly twice longer than in control astrocytes (97.26 ± 16.09 s, $n = 12$, 343 cells) (Fig. 1E). Overall, these data suggest that $A\beta_{1-42}$ affected astrocytic ATP-induced Ca^{2+} dynamics, causing a decrease in the amplitude and a prolonged duration response of the evoked response.

To explore possible sources responsible for the ATP-evoked Ca^{2+} increase in cultured astrocytes and how they are affected by AD-like conditions, we evaluated ATP-evoked Ca^{2+} responses in Krebs buffer without Ca^{2+} and with EGTA (50 µM) [38] and in Krebs buffer with Xestospongin-C (Xe–C, 1 µM, 20 min) [39]; this allowed evaluating the contribution of extracellular Ca^{2+} influx and of Ca^{2+} release from endoplasmic reticulum (ER) through inositol 1,3,5-trisphosphate receptors (IP_3R), respectively. In the absence of extracellular Ca^{2+} (media with EGTA), the amplitude of the ATP-evoked Ca^{2+} response was reduced ($p < 0.05$) in both $A\beta_{1-42}$ (reduction of 54%, 0.34 ± 0.03 a.u., $n = 5$, 100 cells) and control astrocytes (reduction of 36%, 0.56 ± 0.14 a.u., $n = 5$, 147 cells) (Fig. S2). The presence of Xe–C also decreased significantly ($p < 0.05$) the amplitude of ATP-evoked Ca^{2+} response in control conditions (reduction of 73%, Xe–C: 0.78 ± 0.37 a.u., $n = 4$, 110 cells) and also in $A\beta_{1-42}$-treated astrocytes (reduction of 68%, $A\beta_{1-42}$ + Xe–C: 0.34 ± 0.03 a.u., $n = 3$, 140 cells). These data indicate that ATP-evoked increase of intracellular Ca^{2+} levels in the absence or presence of $A\beta_{1-42}$ was mediated from extracellular Ca^{2+} influx and to a highest extent by Ca^{2+} release from ER through IP_3R. The duration of Ca^{2+} response evoked by ATP with these pharmacological approaches (EGTA and Xe–C) was also evaluated. In astrocytes pre-treated with $A\beta_{1-42}$, the duration of response in the presence of EGTA was significantly reduced by 88% ($p < 0.01$, $A\beta_{1-42}$ + EGTA: 21.84 ± 5.82 s, $n = 4$, 70 cells vs. $A\beta_{1-42}$ 188.30 ± 22.73 s, $n = 13$, 342 cells); this effect was lower in control cells, where the presence of EGTA reduced the duration of ATP-evoked Ca^{2+} response by 55% in control astrocytes ($p < 0.05$, EGTA: 43.70 ± 5.44 s, $n = 6$, 143 cells). By contrast, the blockade of IP_3R with Xe–C did not affect the duration of ATP-evoked Ca^{2+} responses in control conditions, although it significantly ($p < 0.05$) reduced by 53% the duration of Ca^{2+} responses in astrocytes pre-treated with $A\beta_{1-42}$ (88.59 ± 19.87 s, $n = 5$, 154 cells). Interestingly, in the presence of Xe–C, the duration of ATP-induced Ca^{2+} responses was similar in astrocytes exposed to $A\beta_{1-42}$ and control astrocytes (Fig. S2); this suggests that Ca^{2+} efflux from ER contributed to the deregulation of Ca^{2+} response duration in AD-like condition.

Effect of $A\beta_{1-42}$ exposure on the contribution of different ATP (P2) receptors to astrocytic Ca^{2+} dynamics

Both ionotropic P_2X_7 receptors (P_2X_7R) and metabotropic P_2Y_1 receptors (P_2Y_1R) are known to contribute to intracellular Ca^{2+} dynamics in response to ATP stimulation in non-pathologic conditions [38, 40–43]. We now investigated how the contribution of each of these receptors for astrocytic Ca^{2+} responses was altered in astrocytes exposed to $A\beta_{1-42}$, using the selective P_2X_7R antagonist JNJ47965567 and the selective P_2Y_1R antagonist MRS2179.

The blockade of ionotropic P_2X_7R, with JNJ47965567 (1 µM) [44], slightly decreased the amplitude (40% reduction, $p = 0.19$) and duration (28% reduction) of ATP-induced Ca^{2+} response in control astrocytes ($p > 0.05$, Fig. 2). However, in $A\beta_{1-42}$-exposed astrocytes the antagonism of P_2X_7R did not affect the amplitude of ATP-induced Ca^{2+} response but reduced its duration by 25% ($A\beta_{1-42}$ + JNJ: 141.20 ± 18.37 s, n = 7, 144 cells vs. JNJ: 70.35 ± 7.79 s, $n = 5$, 101 cells, $p < 0.05$). Notably, in the presence of the P_2X_7R antagonist, the amplitude of ATP-induced Ca^{2+} response was similar in control and $A\beta_{1-42}$-exposed astrocytes; however, the duration of ATP-induced Ca^{2+} response remained higher in $A\beta_{1-42}$-treated astrocytes as compared with control cells (Fig. 2A). These data suggest that P_2X_7R were likely involved in the deregulation of the amplitude of astrocytic Ca^{2+} response evoked by ATP in conditions of $A\beta_{1-42}$ exposure.

The participation of metabotropic P_2Y_1R on ATP-evoked Ca^{2+} response was evaluated using an effective concentration of the selective antagonist MRS2179 (30 µM) [45]. P_2Y_1R blockade significantly decreased by 69% the amplitude (0.75 ± 0.26 a.u., $n = 4$, 81 cells, $p < 0.05$), but increase by 95% the duration of ATP-evoked Ca^{2+} response ($p < 0.05$) in control astrocytes. By contrast, in $A\beta_{1-42}$-exposed astrocytes, P_2Y_1R blockade significantly decreased the amplitude ($p < 0.01$) and slightly reduced ($p > 0.05$) the duration of ATP-evoked Ca^{2+} response, as shown in Fig. 2B. Overall, the results show that both P_2X_7R and P_2Y_1R contributed to the amplitude of ATP-evoked Ca^{2+} response. In addition, P_2Y_1R seemed to have a particular role in regulating the response duration, as its antagonist MRS2179 significantly

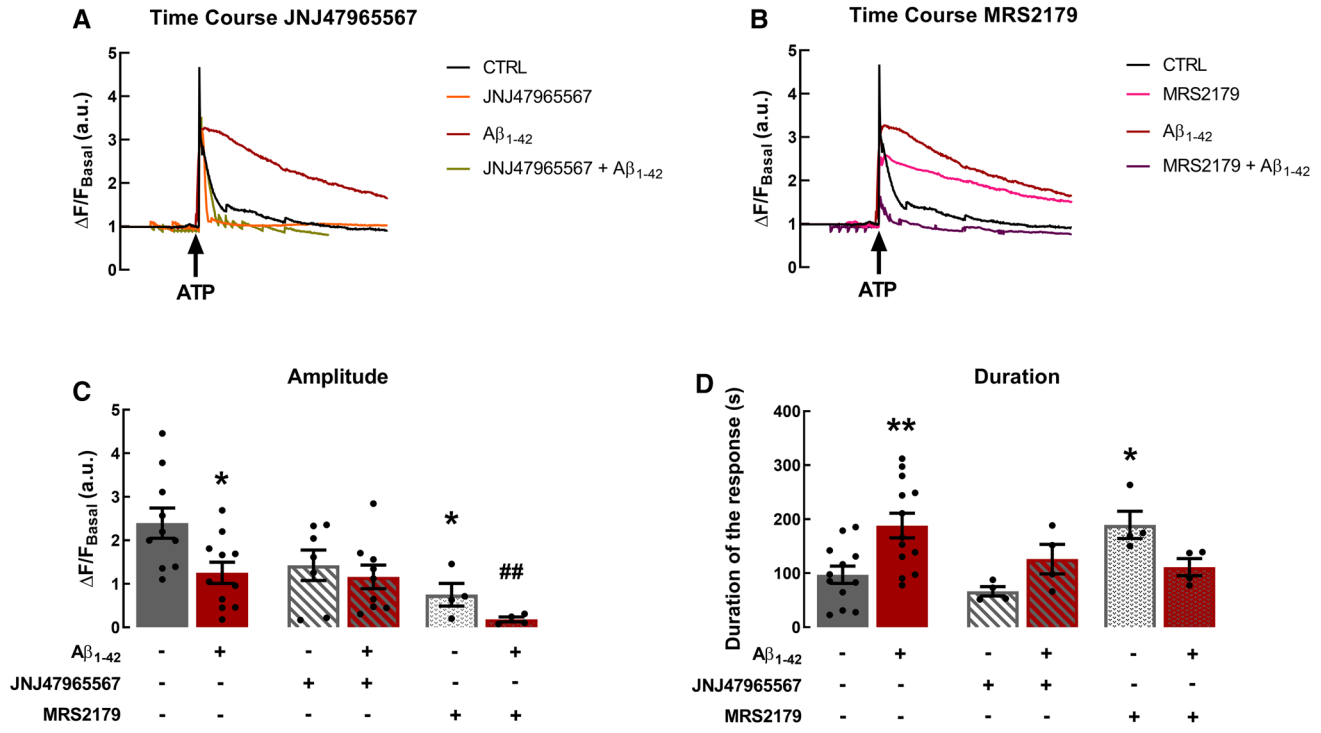

Fig. 2 Involvement of P_2 receptors, P_2X_7R and P_2Y_1R, in the dysregulation of Ca^{2+} dynamics in astrocytes exposed to $A\beta_{1\text{-}42}$. The impact of P_2X_7R and of P_2Y_1R on ATP-evoked Ca^{2+} responses was evaluated using the selective antagonists JNJ7965567 (1 μM) and MRS2179 (30 μM), respectively. Representative time courses of single-cell fluorescence Ca^{2+} imaging in control and $A\beta_{1\text{-}42}$ (1 μM, for 1 h)-exposed astrocytes, stimulated with ATP (100 μM) in the presence JNJ7965567 (**A**) or of MRS2179 (**B**). The bar graphs represent the ATP-evoked Ca^{2+} response amplitude (**C**) and duration (**D**) in astrocytes in the different experimental conditions. The P_2X_7R antagonist did not significantly affect neither the amplitude nor the duration of Ca^{2+} response evoked by ATP in both control and $A\beta_{1\text{-}42}$-exposed astrocytes. P_2Y_1R antagonism significantly decreased the amplitude of Ca^{2+} response evoked by ATP in control and $A\beta_{1\text{-}42}$-exposed astrocytes, whereas it significantly increased the duration of Ca^{2+} response in control cells and slightly reduced the duration of Ca^{2+} response in astrocytes exposed to $A\beta_{1\text{-}42}$. Ca^{2+} oscillations were monitored by single-cell Ca^{2+} fluorescence imaging, being the ATP-evoked Ca^{2+} response amplitude and duration expressed in arbitrary units (a.u.) and in seconds (s), respectively. Data are mean ± SEM of 4–13 independent experiments. $*p<0.05$, $**p<0.01$ as compared to control; $\#\#p<0.01$ as compared $A\beta_{1\text{-}42}$-treated astrocytes, Mann–Whitney test

increased the decay of ATP-evoked $[Ca2+]_i$, i.e., the response duration, in non-pathological conditions (control astrocytes). In astrocytes exposed to $A\beta_{1\text{-}42}$, the blockade of P_2X_7R and of P_2Y_1R restored the duration of ATP-evoked Ca^{2+} response to values similar to control levels, indicating an altered contribution of these receptors under AD-like conditions.

Impact of adenosine A_{2A} receptors on ATP-induced Ca^{2+} dynamics in astrocytes

We have previously shown that $A_{2A}R$ are present in astrocytes and that their blockade has beneficial effects in several brain pathologies, including AD [28, 46–48]. We now investigated the possible involvement of $A_{2A}R$ in ATP-induced Ca^{2+} dynamics in control and $A\beta_{1\text{-}42}$-exposed astrocytes using a selective $A_{2A}R$ antagonist, SCH58261 (Fig. 3A). In the presence of SCH58261 (50 nM) [28], added 15 min before ATP stimulation, the amplitude of Ca^{2+} response was significantly reduced in control conditions (CTRL: 2.40 ± 0.35 a.u. vs. SCH: 1.08 ± 0.23 a.u., $n=4$, 107 cells, $p<0.05$, 55% reduction); whereas in astrocytes pretreated with $A\beta_{1\text{-}42}$ a slight reduction was also observed ($A\beta_{1\text{-}42}$: 1.22 ± 0.23 a.u. vs. $A\beta_{1\text{-}42}$ + SCH: 0.72 ± 0.15 a.u., $p=0.151$, $n=11$, 221 cells, 41% reduction) (Fig. 3B). Curiously, SCH58261 per se increased ($p<0.05$) the duration of ATP-evoked Ca^{2+} response in control cells (CTRL: 97.26 ± 16.06 s vs. SCH: 199.4 ± 36.47 s, $n=3$, 113 cells), while in astrocytes exposed to $A\beta_{1\text{-}42}$ SCH58261 decreased the duration of ATP-evoked Ca^{2+} response by 45% ($p<0.01$, $A\beta_{1\text{-}42}$: 188.30 ± 2.73 s vs. Aβ + SCH 104.30 ± 17.42 s, $n=11$, 211 cells). The duration of ATP-evoked Ca^{2+} response in the presence of SCH58261 in Aβ-treated cells was similar to that observed in control cells; this suggests that $A_{2A}R$ regulate the duration of the ATP-induced Ca^{2+} response and that the $A_{2A}R$ blockade rescued the alterations induced by $A\beta_{1\text{-}42}$ in the duration of ATP-evoked Ca^{2+} response (Fig. 3C).

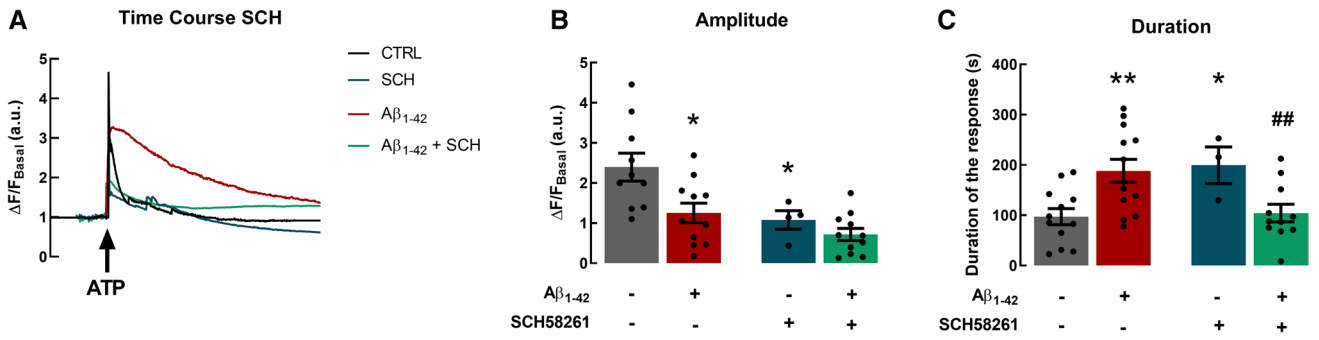

Fig. 3 Adenosine A_{2A} receptors ($A_{2A}R$) regulated astrocytic Ca^{2+} dynamics in control and $A\beta_{1-42}$-exposed astrocytes. $A_{2A}R$ involvement in ATP-evoked Ca^{2+} response was evaluated using the selective antagonist SCH58261 (50 nM). **A** Representative time course of single-cell fluorescence recording of Ca^{2+} dynamics evoked by ATP (100 µM) in the presence or absence SCH58261 in astrocytes pre-exposed to $A\beta_{1-42}$ (1 µM, for 1 h). In control conditions (no $A\beta_{1-42}$ exposure), SCH58261 decreased the amplitude **(B)** of ATP-evoked Ca^{2+} response, but increased the duration of Ca^{2+} response **(C)**. Astrocytes exposed to $A\beta_{1-42}$ and further incubated with SCH58261 did not show differences in the amplitude of ATP-evoked Ca^{2+} response but displayed a significant decrease in the duration of ATP-evoked astrocytic Ca^{2+} response, indicating that $A_{2A}R$ are involved in alterations of astrocytic Ca^{2+} dynamics triggered by $A\beta_{1-42}$ exposure. The amplitude and duration of Ca^{2+} response evoked by ATP were expressed in arbitrary units (a.u.) and seconds (s), respectively. Data are mean ± SEM of 3–12 independent experiments. $*p<0.05$, $**p<0.01$ as compared to control; $\#\#p<0.01$ as compared $A\beta_{1-42}$-treated astrocytes, Mann–Whitney test

Interaction between adenosine A_{2A} receptors and ATP P_2X_7 and P_2Y_1 receptors in astrocytic Ca^{2+} dynamics

In light of the impact of P_2X_7R, P_2Y_1R and $A_{2A}R$ in ATP-evoked Ca^{2+} responses, we investigated a possible functional interaction between these purinergic receptors in the regulation of $[Ca^{2+}]_i$, using cell population Ca^{2+} measurements. The P_2X_7R agonist BzATP (100 µM) [49] increased $\Delta[Ca^{2+}]_i$ by 450.71 ± 45.85 nM in non-treated cells and by 378.40 ± 55.16 nM in $A\beta_{1-42}$-treated astrocytes ($p>0.05$, $n=7$, Fig. 4A). The selective $P_{2X7}R$ antagonist JNJ47965567 (1 µM) reduced the effects BzATP by 92% ($p<0.001$, Fig. 4A). Notably, the selective $A_{2A}R$ antagonist SCH58261 (50 nM) decreased BzATP-induced $\Delta[Ca^{2+}]_i$ to 221.25 ± 44.70 nM in non-treated astrocytes ($p<0.05$, $n=4$–7), whereas in astrocytes treated with $A\beta_{1-42}$, SCH58261 did not affected BzATP-evoked $\Delta[Ca^{2+}]_i$ ($p>0.05$, Fig. 4A). This indicates an involvement of $A_{2A}R$ in the regulation of $[Ca^{2+}]_i$ increases mediated by

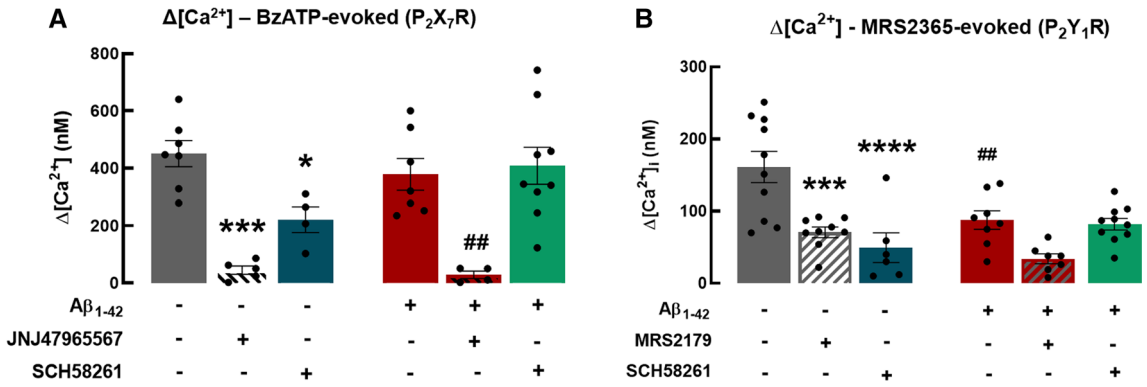

Fig. 4 Interaction between $A_{2A}R$ and P_2 receptors (P_2X_7R and P_2Y_1R) in the regulation of Ca^{2+} responses in control and $A\beta_{1-42}$-exposed astrocytes. Intracellular Ca^{2+} increases ($\Delta[Ca^{2+}]_i$) evoked by the agonists of $P_{2X7}R$, BzATP (100 µM, **A**) and of $P_{2Y1}R$, MRS2365 (10 nM, **B**) in control and $A\beta_{1-42}$ (1 µM, for 1 h)-treated astrocytes. Both agonists increased the $\Delta[Ca^{2+}]_i$ in control and in $A\beta_{1-42}$-treated astrocytes, and these effects were attenuated by their respective antagonists JNJ7965567 (1 µM) and MRS2179 (30 µM). Although $\Delta[Ca^{2+}]_i$ evoked by BzATP was similar in control and $A\beta_{1-42}$-exposed astrocytes, the $\Delta[Ca^{2+}]_i$ evoked by MRS2365 in $A\beta_{1-42}$-treated astrocytes was significant lower than these observed in control astrocytes. The $A_{2A}R$ antagonist SCH58261 (50 nM) decreased the $\Delta[Ca^{2+}]_i$ evoked by either BzATP or MRS2365 in control astrocytes, but not in $A\beta_{1-42}$-exposed astrocytes. Data are mean ± SEM of 4–10 independent experiments. $*p<0.05$, $***p<0.001$, $****p<0.0001$ as compared to control, one-way ANOVA followed by Dunnett's post hoc test; $\#\#p<0.01$ as compared $A\beta_{1-42}$-treated astrocytes, two-way ANOVA, post hoc Tukey's test

P_2X_7R in control astrocytes, which disappears in $A\beta_{1-42}$-treated astrocytes.

The P_2Y_1R agonist MRS2365 (10 nM) [50] increased $\Delta[Ca^{2+}]_i$ by 161.10 ± 21.80 nM in non-treated cells and this effect was significantly lower in $A\beta_{1-42}$-treated astrocytes ($\Delta[Ca^{2+}]_i$ = 87.75 ± 12.86 nM, $p < 0.05$, n = 8–10, Fig. 4B). The selective $P_{2Y1}R$ antagonist MRS2179 (10 μM) significantly reduced by 56% and 61% the MRS2365-induced $\Delta[Ca^{2+}]_i$ in non-treated and in $A\beta_{1-42}$-treated astrocytes, respectively ($p < 0.001$, n = 9–10). The P_2Y_1R-mediated Ca^{2+} response was also significantly reduced in cells treated with the $A_{2A}R$ selective antagonist SCH58261 in control conditions ($p < 0.001$, n = 6–10), but SCH58261 was devoid of effects in astrocytes treated with $A\beta_{1-42}$ (Fig. 4B). These data suggest a different role of $A_{2A}R$ in the regulation of astrocytic Ca^{2+} dynamics in non-pathologic and in early AD-like conditions.

Considering the functional observations indicating a different effect of P_2X_7R and P_2Y_1R in $[Ca^{2+}]_i$ regulation in control and AD-conditions, we next probed for alterations of the density of these receptors by Western Blot between control and AD-like astrocytes. Astrocytes treated with $A\beta_{1-42}$ exhibited P_2X_7R levels similar to these of non-treated cells ($p > 0.05$, n = 14, Fig. 5A). By contrast, the density of P_2Y_1R was higher in $A\beta_{1-42}$-treated astrocytes as compared to control ($p < 0.05$, n = 10), and this effect was not prevented by the $A_{2A}R$ antagonist SCH58261 ($p > 0.05$, n = 10, Fig. 5B). Altogether, these data suggest that $A_{2A}R$ modify the impact of P_2X_7R and of P_2Y_1R in $[Ca^{2+}]_i$ through a mechanism independent of the control of their density.

P_2X_7 receptors modulate astrocytic Ca^{2+} dynamics mediated by P_2Y_1 receptor activation

The results described above showing a similar involvement of $A_{2A}R$ in the modulation of $[Ca^{2+}]_i$ evoked by P_2X_7R and P_2Y_1R activation and a differential involvement of these receptors in ATP-induced $[Ca^{2+}]_i$ responses, lead us to hypothesize a functional interaction between P_2X_7R and P_2Y_1R. The P_2Y_1R selective antagonist MRS2179 (30 μM) did not modify $[Ca^{2+}]_i$ responses triggered by the P_2X_7R agonist BzATP (100 μM) neither in control nor in $A\beta_{1-42}$-treated astrocytes ($p > 0.05$, Fig. 6A). In contrast, the P_2X_7R antagonist JNJ7965567 (1 μM) significantly decreased by 67% ($p < 0.01$, n = 6–10) $\Delta[Ca^{2+}]_i$ responses triggered by the P_2Y_1R agonist MRS2365 (10 nM) in control astrocytes but not in $A\beta_{1-42}$-treated astrocytes (Fig. 6B). Furthermore, P_2X_7R blockade significantly increased ($p < 0.05$) P_2Y_1R density in control conditions, but not in $A\beta_{1-42}$-treated astrocytes (Fig. S3). In contrast, the selective antagonist of P_2Y_1R, MRS2179 (30 μM) did not affect either their own density (Fig. S4A) nor P_2X_7R density (Fig. S4B) and the non-selective antagonists of P_2X, PPADS (10 μM) [40] or of P_2Y, Reactive Blue-2 (2 μM) [51] were also devoid of effects on the densities of P_2Y_1R (Fig. S4A) or P_2X_7R (Fig. S4B). These results indicate that the selective manipulation of P_2X_7R modulates P_2Y_1R-mediated $[Ca^{2+}]_i$ response in

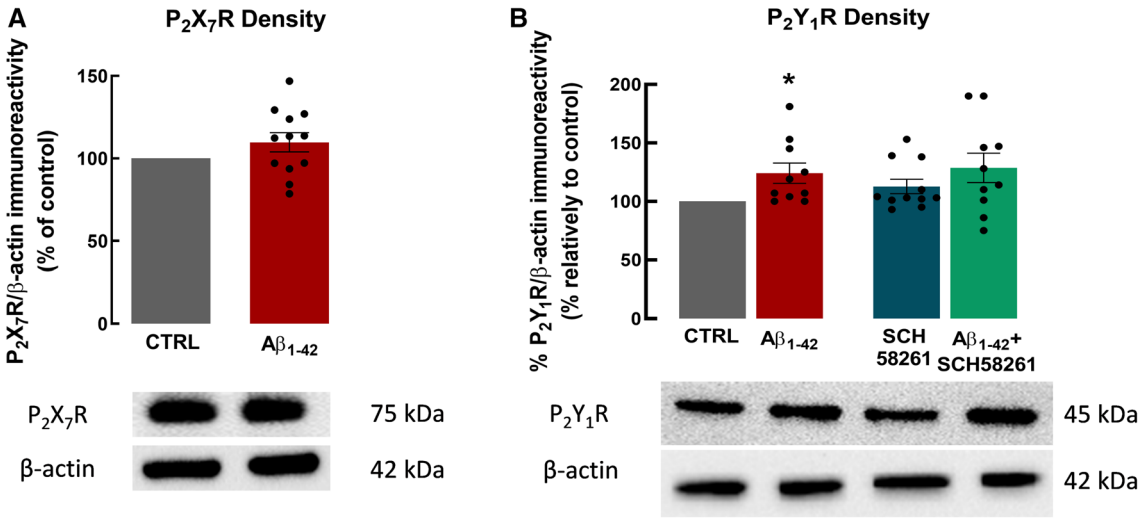

Fig. 5 Impact of $A\beta_{1-42}$ on the densities of P_2X_7R and P_2Y_1R in astrocytes: regulation by $A_{2A}R$. The densities of P_2X_7R (**A**) and P_2Y_1R (**B**) were evaluated in astrocytes control (CTRL) and in astrocytes exposed to $A\beta_{1-42}$. (1 μM, for 24 h). $A\beta_{1-42}$ did not affect P_2X_7R levels, but significantly increased P_2Y_1R levels and this increase was prevented by the selective $A_{2A}R$ antagonist SCH58261 (50 nM, co-incubated with $A\beta_{1-42}$ for 24 h). Graph bars represent the ratio of immunoreactivities between **A** P_2X_7R and β-actin (used as a loading protein control) or between **B** P_2Y_1R and β-actin and were expressed as a percentage of values of control cells. Representative immunoblotting of $P_{2X7}R$ (75 kDa), $P_{2Y1}R$ (45 kDa) and β-actin (42 kDa) are also shown. Data are mean ± S.E.M. of 10–12 independent experiments. *$p < 0.05$ as compared to control (100%), one sample t test

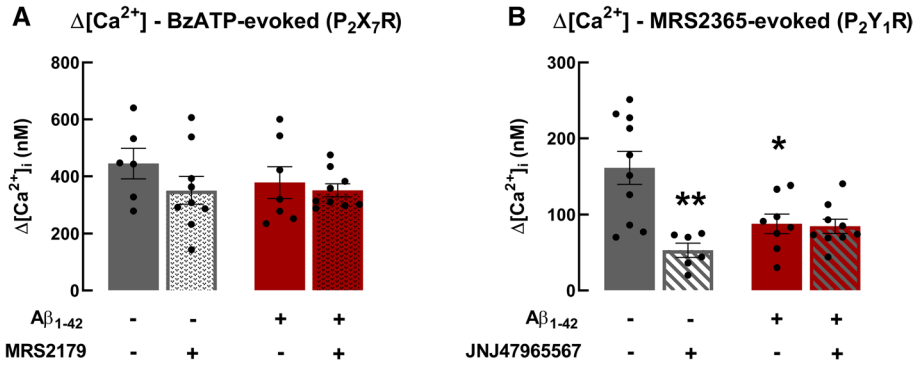

Fig. 6 Interaction between P_2X_7R- and P_2Y_1R-induced Ca^{2+} responses in control and $A\beta_{1\text{-}42}$-exposed astrocytes. Intracellular Ca^{2+} increases ($\Delta[Ca^{2+}]_i$) were evoked by the agonists of P_2X_7R, B_ZATP (100 μM, **A**) and of P_2Y_1R, MRS2365 (10 nM, **B**) in control and in $A\beta_{1\text{-}42}$ (1 μM, for 1 h)-treated astrocytes. The putative interaction of P_2X_7R and of P_2Y_1R on $\Delta[Ca^{2+}]_i$ was evaluated by stimulating with **A** P_2X_7R agonist in the presence of P_2Y_1R antagonist, MRS2179 30 μM, or **B** with P_2Y_1R agonist in the presence of P_2X_7R antagonist, JNJ7965567 1 μM, in astrocytes without or in the presence of $A\beta_{1\text{-}42}$. P_2Y_1R did not modulate $\Delta[Ca^{2+}]_i$ evoked by P_2X_7R activation, whereas P_2X_7R modulate $\Delta[Ca^{2+}]_i$ evoked by P_2Y_1R activation in control cells but not in $A\beta_{1\text{-}42}$-exposed astrocytes. Data are mean ± SEM of 6–10 independent experiments. $^*p < 0.05$, $^{**}p < 0.01$ as compared to control, one-way ANOVA followed by Dunnett's post hoc test

non-pathologic conditions but not in the presence of $A\beta_{1\text{-}42}$, whereas P_2Y_1R did not affect P_2X_7R-mediated $[Ca^{2+}]_i$ responses in astrocytes.

PKA is involved in P_2X_7R- and P_2Y_1R-mediated astrocytic $[Ca^{2+}]_i$ increases in non-pathologic conditions

Since $A_{2A}R$ are canonically coupled with activation of cAMP-dependent transducing pathways, we next investigated if PKA activity affected the P_2X_7R- or P_2Y_1R-induced Ca^{2+} responses. As shown in Fig. 7A, the PKA inhibitor H-89 (10 μM) [52] decreased by 61% the $\Delta[Ca^{2+}]_i$ response induced by P_2X_7R in non-pathological conditions (CTRL: 444.83 ± 53.80 nM, H-89: 173.29 ± 33.29 nM, $n = 6$–7, $p < 0.01$); in contrast, this effect was absent in the presence of $A\beta_{1\text{-}42}$ ($p > 0.05$, $n = 7$–8). Similarly, PKA inhibition also decreased by 43% the P_2Y_1R-induced $[Ca^{2+}]_i$ response in non-pathological conditions ($p < 0.05$, $n = 8$–10); in contrast, the treatment with H-89 was devoid of effects in $A\beta_{1\text{-}42}$-treated astrocytes, as shown in Fig. 7B. These data further re-inforce that $A_{2A}R$ coupled to PKA activation control both P_2X_7R- and P_2Y_1R-induced $[Ca^{2+}]_i$ responses in control conditions and this effect is lost after exposure to $A\beta_{1\text{-}42}$.

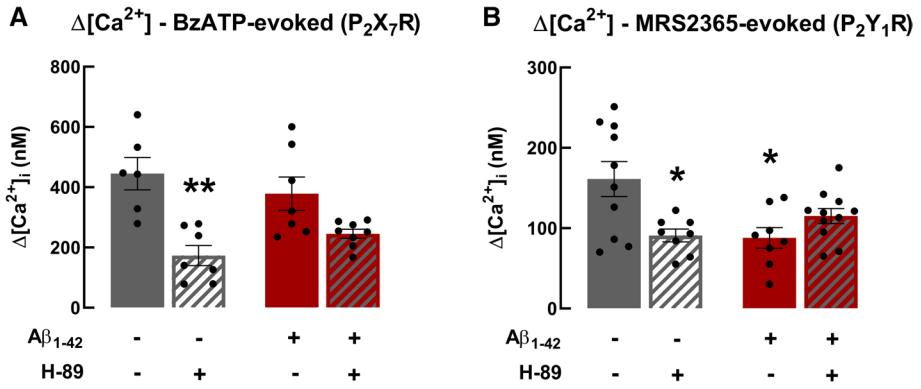

Fig. 7 Impact of a protein kinase A (PKA) inhibitor on P_2X_7R- and P_2Y_1R-induced Ca^{2+} responses in control and $A\beta_{1\text{-}42}$-exposed astrocytes. In astrocytes exposed to $A\beta_{1\text{-}42}$ (1 μM for 1 h) or not, the intracellular Ca^{2+} increases ($\Delta[Ca^{2+}]_i$) was evaluated by stimulating astrocytes with 100 μM BzATP (**A**) or 10 nM MRS2365 (**B**) in the absence or presence of the PKA inhibitor H-89 (10 μM). H-89 significantly decreased the $\Delta[Ca^{2+}]_i$ evoked by the agonists of $P_{2X7}R$ and $P_{2Y1}R$ in control astrocytes, but had no significant effect on $\Delta[Ca^{2+}]_i$ evoked by these agonists in astrocytes exposed to $A\beta_{1\text{-}42}$. Data are mean ± SEM of 6–11 independent experiments. $^*p < 0.05$, $^{**}p < 0.01$ as compared to control, one-way ANOVA followed by Dunnett's post hoc test

Discussion

The present results identify a hitherto unrecognized functional interaction between adenosine A_{2A} receptors ($A_{2A}R$) and P_2X_7 (P_2x_7R) and P_2Y_1 receptors (P_2Y_1R) in the control of intracellular Ca^{2+} responses in cultured astrocytes. Thus, ATP triggered an astrocytic Ca^{2+} response through a parallel activation of P_2X_7R and P_2Y_1R, with P_2X_7R potentiating P_2Y_1R-mediated effects, and these ATP responses were fine-tuned by $A_{2A}R$. Notably, amyloid-β peptides (Aβ) exposure, to mimic the early phase of Alzheimer's disease (AD), altered the purinergic modulation of astrocytes: (i) astrocytes became less responsive to a danger signal, such as ATP; (ii) astrocytes lost the fine tuning of Ca^{2+}-driven adaptive responses afforded by the tight interplay between different signaling components of these purinergic receptors.

The first major conclusion of the present study is the basic pharmacological characterization of the P_2R involved in ATP-induced Ca^{2+}-responses in astrocytes, as involving P_2X_7R and P_2Y_1R. This is in accordance with the previously identified presence and major role of P_2Y_1R as well as of P_2X_7R in the control of astrocytic Ca^{2+} responses [e.g., 40, 43, 49, 53–55], with P_2X_7R mediating Ca^{2+} entry from extracellular space, whereas P_2Y_1R allow the Ca^{2+} efflux from intracellular stores [56–58]. We now confirmed that metabotropic P_2Y_1R mainly controlled the amplitude of Ca^{2+} response [37, 43], whereas the plateau component, related with response duration, is intrinsically associated with the ionotropic P_2X_7R [40–42, 59]. However, it had not yet been previously explored if ionotropic and metabotropic P_2R interacted in the control of astrocytic Ca^{2+} responses. We now observed that P_2X_7R blockade attenuated P_2Y_1R-induced Ca^{2+} responses, whereas P_2Y_1R blockade did not affect P_2X_7R-induced Ca^{2+} responses. This suggests a primordial role of P_2X_7R in the adaption of the astrocytic purinergic system, as previously hinted based on the analysis of adaptive P_2R gene expression [60]. This novel aspect of the interplay between different purinoceptors in defining astrocytic Ca^{2+} responses is further heralded by the observed ability of adenosine $A_{2A}R$ to control P_2R-induced Ca^{2+} responses in astrocytes. Thus, $A_{2A}R$ blockade decreased both P_2X_7R- and P_2Y_1R-mediated responses, as also observed in other biological systems [42, 61]. This $A_{2A}R$ potentiation of P_2R responses involved the recruitment of protein kinase A, the canonical transducing system of $A_{2A}R$ [62], namely in astrocytes [32, 52, 63]. Overall, this characterization of the crosstalk between different purinoceptors emphasizes the need to evaluate the impact of the integrated purinome rather than the effect of individual receptors to understand the role of the purinergic system [reviewed in 21]. More importantly, the observed interaction between P_2R indicates that the overall purinergic system is involved in the definition of Ca^{2+} responses in astrocytes: ATP directly triggers Ca^{2+} responses with a main engagement of P_2Y_1R [64], bolstered by P_2X_7R co-activation; furthermore, this P_2R-mediated response is further enhanced likely due to the extracellular conversion of ATP into adenosine and subsequent $A_{2A}R$ activation.

Ca^{2+} responses in astrocytes are currently understood as a major mechanism of astrocytic integrative properties to coordinate neuronal networks [34, 65, 66]. Thus, astrocytes form a second network of integrative communication over neuronal networks: each astrocyte covers numerous synapses [67], with astrocytes sensing synaptic activity and responding with localized Ca^{2+} responses in their processes [e.g., 68, 69]; this can result in overall Ca^{2+} responses that can propagate in the form of Ca^{2+} waves across different astrocytes to influence synaptic activity throughout the network [65, 70]. Thus, the amplitude and duration of these Ca^{2+} responses need to be tightly fine-tuned to ensure a proper integrative information capacity by the astrocytic network. In fact, either depressed or exacerbated Ca^{2+} responses have been reported to be associated with abnormal information processing by neuronal networks [reviewed in 34, 71]. This emphasizes the need of a proper integrative ability rather than only increases or decreases of Ca^{2+} responses for normal brain function. In this context, more than the recognition of the involvement of ATP in mounting these astrocytic Ca^{2+} responses, it is this intricate crosstalk between $A_{2A}R$ and P_2R that emerges as particularly relevant to fine-tune astrocytic Ca^{2+} responses.

The main question explored in this study was to evaluate the modification of this purinergic crosstalk in the control of astrocytic calcium transients in early AD, using an experimental model based on the exposure to soluble (monomers and oligomers) Aβ that we have previously shown to mimics early features of AD in rodents [e.g., 26]. We focused on studying the impact of Aβ on astrocytic calcium transients induced by ATP, a major danger signal in the brain [72], namely released from astrocytes exposed to Aβ [30], with particular attention to alterations of the integrative purinergic signaling. The focus was on alterations of astrocytic Ca^{2+} responses in early AD, since most of the previous descriptions of altered astrocytic Ca^{2+} responses in AD models were made in more advanced phases of AD, with a particular focus on modifications near Aβ plaques [73, 74], which are not yet present at the onset of memory deficits caused by exposure to soluble Aβ [26]. Indeed, several previous studies have already documented a spatio-temporal remodeling of Ca^{2+} signaling in astrocytes with the evolution of pathology in different AD models [reviewed in 34, 35]. Compatible with the direct effects of Aβ on astrocytes [75–77], we observed that Aβ triggered a slightly increase of

basal Ca^{2+} levels in astrocytes. However, the impact of Aβ was far more evident on the pattern of ATP-induced Ca^{2+} responses in astrocytes, as previously observed by others [78]. We now detailed the profile of this Aβ-induced effect and concluded that the peak (amplitude) of Ca^{2+} response of ATP was lower, but the duration, i.e., the time of decay towards basal $[Ca^{2+}]_i$ levels, was significantly increased in Aβ-treated astrocytes compared to control astrocytes. This increased duration of ATP-induced Ca^{2+} responses can be explained by a longer Ca^{2+} efflux from internal stores or extracellular Ca^{2+} influx or by alterations in extruding/buffering Ca^{2+} levels [reviewed in 79], which we reported here to be the pathways involved in astrocytic Ca^{2+} response evoked by ATP (see supplementary data). This prompts the conclusion that Aβ affect the ability of astrocytes to handle Ca^{2+} oscillations, namely due to an abnormal ER-mediated Ca^{2+} efflux, compatible with the ability of Aβ oligomers to cause ER stress and disrupt Ca^{2+} homeostasis [39, 80]. In spite of this concluded impact of Aβ on ER-related Ca^{2+} management, we now observed that the ability of P_2Y_1R to control astrocytic Ca^{2+} responses was essentially preserved: thus, the effect of the P_2Y_1R agonist was preserved and a P_2Y_1R antagonist attenuated ATP-induced Ca^{2+} responses in astrocytes exposed to $Aβ_{1-42}$, as also reported to occur in astrocytes surrounding Aβ plaques [66, 73]. Likewise, the impact of P_2X_7R agonists and the contribution of P_2X_7R for ATP-mediated astrocytic Ca^{2+} responses was not altered upon Aβ exposure. Notably, the most striking alteration caused by Aβ exposure was the disappearance of the cross-talk between purinergic receptors. Thus, Aβ exposure eliminated the P_2X_7R-mediated potentiation of P_2Y_1R and the $A_{2A}R$ modulation of P_2R-induced Ca^{2+} responses. Therefore, although each P_2R maintained its ability to control Ca^{2+} responses in early AD, purinoceptors can no longer orchestrate a coordinated response to fine-tune Ca^{2+}-responses. This prompts the hypothesis that the Aβ-induced purinergic incoordination may contribute for the abnormal neuron-glia communication in early AD.

It is important to note that the present study focused on the characterization of the interplay between P_2X_7R and P_2Y1R and the control of ATP-induced astrocytic Ca^{2+} responses and how this is affected in early AD-like conditions. It remains to be investigated how Aβ might affect the ability of the different purinergic receptors to control the multiple functions exerted by astrocytes to influence neuronal function. This is most evident for astrocytic $A_{2A}R$, which density increases upon exposure to Aβ [28] and controls multiple astrocytic responses ranging from the astrocytic membrane potential [31] to connexins [30] to the release of inflammatory mediators [63] and of gliotransmitters [30, 81], through a complex signaling involving biochemical and transcriptional alterations in astrocytes [82]. Thus, the Aβ-induced increase of $A_{2A}R$ levels may engage other astrocytic mediated responses to interfere with the impact of Aβ on astrocytic Ca^{2+} responses as well as on brain dysfunction [29, 83], which ought to be explored in future studies.

The present findings show that the integrative purinergic modulation of astrocytic Ca^{2+} responses is lost upon exposure to Aβ. This indicates that purinergic dysfunction may contribute to abnormal information processing in early AD, not only due to abnormal modulation of synaptic transmission [e.g., 27, 84, 85; reviewed in 86]), but also due to a disrupted integrative modulation of astrocytic Ca^{2+} responses, as now documented.

Supplementary Information The online version contains supplementary material available at https://doi.org/10.1007/s00018-022-04492-y.

Author contributions LD, RD and DM performed astrocytes cultures and Ca^{2+} measurements. Data analysis of live-cell Ca^{2+} imaging and of intracellular Ca^{2+} concentration were done by LD, RD and AT. Western blot assays were carried out by LD and RD. Experimental planning, data interpretation, and manuscript writing were ensured by RAC and PA.

Funding This work was supported by La Caixa Foundation (HP17/00523), Centro 2020 (CENTRO-01–0145-FEDER-000008:BrainHealth 2020 and CENTRO-01–0246-FEDER-000010) and FCT (PTDC/MED-NEU/31274/2017 and UIDB/04539/2020); PhD grants were awarded to Liliana Dias (SFRH/BD/147159/2019) and Daniela Madeira (SFRH/BD/139334/2018).

Data availability The data that support the findings of this study are available from the corresponding author upon reasonable request.

Declarations

Conflict of interest Rodrigo A. Cunha is a scientific advisor of the Institute for Scientific Information on Coffee (ISIC).

Ethics approval This study was approved by the ORBEA_128_2015/04122015 and certified by Direção Geral de Alimentação e Veterinária (DGAV; 0421/000/000/2016 Ref 014420).

References

1. Sofroniew MV, Vinters HV (2010) Astrocytes: biology and pathology. Acta Neuropathol 119(1):7–35. https://doi.org/10.1007/s00401-009-0619-8
2. Santello M, Toni N, Volterra A (2019) Astrocyte function from information processing to cognition and cognitive impairment. Nat Neurosci 22(2):154–166. https://doi.org/10.1038/s41593-018-0325-8
3. Wang DD, Bordey A (2008) The astrocyte odyssey. Prog Neurobiol 86(4):342–367. https://doi.org/10.1016/j.pneurobio.2008.09.015
4. Araque A, Carmignoto G, Haydon PG, Oliet HR, Robitaille R, Volterra A (2014) Gliotransmitters travel in time and space. Neuron 81(4):728–739. https://doi.org/10.1016/j.neuron.2014.02.007

5. Allen NJ, Lyons DA (2018) Glia as architects of central nervous system formation and function. Science 362(6411):181–185. https://doi.org/10.1126/science.aat0473
6. Guerra-Gomes S, Sousa N, Pinto L, Oliveira JF (2018) Functional roles of astrocyte calcium elevations: from synapses to behavior. Front Cell Neurosci 11:427. https://doi.org/10.3389/fncel.2017.00427
7. Volterra A, Meldolesi J (2005) Astrocytes, from brain glue to communication elements: the revolution continues. Nat Rev Neurosci 6(8):626–640. https://doi.org/10.1038/nrn1722
8. Bazargani N, Attwell D (2016) Astrocyte calcium signaling: the third wave. Nat Neurosci 19(2):182–189. https://doi.org/10.1038/nn.4201
9. Verkhratsky A, Matteoli M, Parpura V, Mothet JP, Zorec R (2016) Astrocytes as secretory cells of the central nervous system: idiosyncrasies of vesicular secretion. EMBO J 35(3):239–257. https://doi.org/10.15252/embj.201592705
10. Araque A, Marti ED, Perea G, Arellano JI, Bun W (2002) Synaptically released acetylcholine evokes Ca^{2+} elevations in astrocytes in hippocampal slices. J Neurosci 22(7):2443–2450. https://doi.org/10.1523/JNEUROSCI.22-07-02443.2002
11. Haas B, Schipke CG, Peters O, Sohl G, Willecke K, Kettenmann H (2006) Activity-dependent ATP-waves in the mouse neocortex are independent from astrocytic calcium waves. Cereb Cortex 16(2):237–246. https://doi.org/10.1093/cercor/bhi101
12. Sun MY, Devaraju P, Xie AX, Holman I, Samones E, Murphy TR, Fiacco TA (2014) Astrocyte calcium microdomains are inhibited by bafilomycin A1 and cannot be replicated by low-level Schaffer collateral stimulation in situ. Cell Calcium 55(1):1–16. https://doi.org/10.1016/j.ceca.2013.10.004
13. Ma Z, Stork T, Bergles DE, Freeman MR (2016) Neuromodulators signal through astrocytes to alter neural circuit activity and behaviour. Nature 539(7629):428–432. https://doi.org/10.1038/nature20145
14. Parpura V, Heneka MT, Montana V, Oliet SH, Schousboe A, Haydon PG, Stout RF Jr, Spray DC, Reichenbach A, Pannicke T, Pekny M, Pekna M, Zorec R, Verkhratsky A (2012) Glial cells in (patho)physiology. J Neurochem 121(1):4–27. https://doi.org/10.1111/j.1471-4159.2012.07664.x
15. Khakh BS, Sofroniew MV (2015) Diversity of astrocyte functions and phenotypes in neural circuits. Nat Neurosci 18(7):942–952. https://doi.org/10.1038/nn.4043
16. Verkhratsky A, Orkand RK, Kettenmann H (1998) Glial calcium: homeostasis and signaling function. Physiol Rev 78(1):99–141. https://doi.org/10.1152/physrev.1998.78.1.99
17. Jeremic A, Jeftinija K, Stevanovic J, Glavaski A, Jeftinija S (2001) ATP stimulates calcium-dependent glutamate release from cultured astrocytes. J Neurochem 77(2):664–675. https://doi.org/10.1046/j.1471-4159.2001.00272.x
18. Vardjan N, Parpura V, Zorec R (2016) Loose excitation-secretion coupling in astrocytes. Glia 64(5):655–667. https://doi.org/10.1002/glia.22920
19. Sherwood MW, Arizono M, Hisatsune C, Bannai H, Ebisui E, Sherwood JL, Panatier A, Oliet SH, Mikoshiba K (2017) Astrocytic IP_3Rs: contribution to Ca^{2+} signalling and hippocampal LTP. Glia 65(3):502–513. https://doi.org/10.1002/glia.23107
20. Boison D, Chen JF, Fredholm BB (2010) Adenosine signaling and function in glial cells. Cell Death Differ 17(7):1071–1082. https://doi.org/10.1038/cdd.2009.131
21. Agostinho P, Madeira D, Dias L, Simões AP, Cunha RA, Canas PM (2020) Purinergic signaling orchestrating neuron-glia communication. Pharmacol Res 162:105253. https://doi.org/10.1016/j.phrs.2020.105253
22. Gomes CV, Kaster MP, Tomé AR, Agostinho PM, Cunha RA (2011) Adenosine receptors and brain diseases: neuroprotection and neurodegeneration. Biochim Biophys Acta 1808(5):1380–1399. https://doi.org/10.1016/j.bbamem.2010.12.001
23. Lopes CR, Cunha RA, Agostinho P (2021) Astrocytes and adenosine A_{2A} receptors: active players in Alzheimer's disease. Front Neurosci 15:666710. https://doi.org/10.3389/fnins.2021.666710
24. Li P, Rial D, Canas PM, Yoo J, Li W, Zhou X, Wang Y, van Westen GJ, Payen MP, Augusto E, Gonçalves N, Tomé AR, Li Z, Wu Z, Hou X, Zhou Y, IJzerman AP, Boyden ES, Cunha RA, Qu J, Chen JF (2015) Optogenetic activation of intracellular adenosine A_{2A} receptor signaling in the hippocampus is sufficient to trigger CREB phosphorylation and impair memory. Mol Psychiatry 20(11):1339–1349. https://doi.org/10.1038/mp.2014.182
25. Stine WB Jr, Dahlgre KN, Krafft GA, LaDu MJ (2003) In vitro characterization of conditions for amyloid-beta peptide oligomerization and fibrillogenesis. J Biol Chem 278(13):11612–11622. https://doi.org/10.1074/jbc.M210207200
26. Canas PM, Porciúncula LO, Cunha GM, Silva CG, Machado NJ, Oliveira JM, Oliveira CR, Cunha RA (2009) Adenosine A_{2A} receptor blockade prevents synaptotoxicity and memory dysfunction caused by beta-amyloid peptides via p38 mitogen-activated protein kinase pathway. J Neurosci 29(47):14741–14751. https://doi.org/10.1523/JNEUROSCI.3728-09.2009
27. Viana-da-Silva S, Haberl MG, Zhang P, Bethge P, Lemos C, Gonçalves N, Gorlewicz A, Malezieux M, Gonçalves FQ, Grosjean N, Blanchet C, Frick A, Nägerl UV, Cunha RA, Mulle C (2016) Early synaptic deficits in the APP/PS1 mouse model of Alzheimer's disease involve neuronal adenosine A_{2A} receptors. Nat Commun 7:11915. https://doi.org/10.1038/ncomms11915
28. Matos M, Augusto E, Machado NJ, dos Santos-Rodrigues A, Cunha RA, Agostinho P (2012) Astrocytic adenosine A_{2A} receptors control the amyloid-β peptide-induced decrease of glutamate uptake. J Alzheimers Dis 31(3):555–567. https://doi.org/10.3233/JAD-2012-120469
29. Orr AG, Hsiao EC, Wang MM, Ho K, Kim DH, Wang X, Guo W, Kang J, Yu GQ, Adame A, Devidze N, Dubal DB, Masliah E, Conklin BR, Mucke L (2015) Astrocytic adenosine receptor A_{2A} and G_s-coupled signaling regulate memory. Nat Neurosci 18(3):423–434. https://doi.org/10.1038/nn.3930
30. Madeira D, Dias L, Santos P, Cunha RA, Canas PM, Agostinho P (2021) Association between adenosine A_{2A} receptors and connexin 43 regulates hemichannels activity and ATP release in astrocytes exposed to amyloid-β peptides. Mol Neurobiol 58(12):6232–6248. https://doi.org/10.1007/s12035-021-02538-z
31. Matos M, Augusto E, Agostinho P, Cunha RA, Chen J (2013) Antagonistic Interaction between Adenosine A_{2A} receptors and Na^+/K^+-ATPase-α_2 controlling glutamate uptake in astrocytes. J Neurosci 33(47):18492–18502. https://doi.org/10.1523/JNEUROSCI.1828-13.2013
32. Matos M, Augusto E, Santos-Rodrigues AD, Schwarzschild MA, Chen JF, Cunha RA, Agostinho P (2012) Adenosine A_{2A} receptors modulate glutamate uptake in cultured astrocytes and gliosomes. Glia 60(5):702–716. https://doi.org/10.1002/glia.22290
33. Abramov AY, Canevari L, Duchen MR (2003) Changes in intracellular calcium and glutathione in astrocytes as the primary mechanism of amyloid neurotoxicity. J Neurosci 23(12):5088–5095. https://doi.org/10.1523/JNEUROSCI.23-12-05088.2003
34. Lim D, Rodríguez-Arellano JJ, Parpura V, Zorec R, Zeidán-Chuliá F, Genazzani AA, Verkhratsky A (2016) Calcium signalling toolkits in astrocytes and spatio-temporal progression of Alzheimer's disease. Curr Alzheimer Res 13(4):359–369. https://doi.org/10.2174/1567205013666151116130104
35. Verkhratsky A (2019) Astroglial calcium signaling in aging and Alzheimer's disease. Cold Spring Harb Perspect Biol 11(7):a035188. https://doi.org/10.1101/cshperspect.a035188

36. Piacentini R, Li Puma DD, Mainardi M, Lazzarino G, Tavazzi B, Arancio O, Grassi C (2017) Reduced gliotransmitter release from astrocytes mediates tau-induced synaptic dysfunction in cultured hippocampal neurons. Glia 65(8):1302–1316. https://doi.org/10.1002/glia.23163
37. Jacob PF, Vaz SH, Ribeiro JA, Sebastião AM (2014) P2Y1 receptor inhibits GABA transport through a calcium signalling-dependent mechanism in rat cortical astrocytes. Glia 62(8):1211–1226. https://doi.org/10.1002/glia.22673
38. Alberdi E, Wyssenbach A, Alberdi M, Sánchez-Gómez MV, Cavaliere F, Rodríguez JJ, Verkhratsky A, Matute C (2013) Ca^{2+}-dependent endoplasmic reticulum stress correlates with astrogliosis in oligomeric amyloid β-treated astrocytes and in a model of Alzheimer's disease. Aging Cell 12(2):292–302. https://doi.org/10.1111/acel.12054
39. Ferreiro E, Resende R, Costa R, Oliveira CR, Pereira CM (2006) An endoplasmic-reticulum-specific apoptotic pathway is involved in prion and amyloid-beta peptides neurotoxicity. Neurobiol Dis 23(3):669–678. https://doi.org/10.1016/j.nbd.2006.05.011
40. Fumagalli M, Brambilla R, D'Ambrosi N, Volonté C, Matteoli M, Verderio C, Abbracchio MP (2003) Nucleotide-mediated calcium signaling in rat cortical astrocytes: role of P2X and P2Y receptors. Glia 43(3):218–303. https://doi.org/10.1002/glia.10248
41. Nobile M, Monaldi I, Alloisio S, Cugnoli C, Ferroni S (2003) ATP-induced, sustained calcium signalling in cultured rat cortical astrocytes: evidence for a non-capacitative, P2X7-like-mediated calcium entry. FEBS Lett 538(1–3):71–76. https://doi.org/10.1016/s0014-5793(03)00129-7
42. Alloisio S, Cugnoli C, Ferroni S, Nobile M (2004) Differential modulation of ATP-induced calcium signalling by A1 and A2 adenosine receptors in cultured cortical astrocytes. Br J Pharmacol 141(6):935–942. https://doi.org/10.1038/sj.bjp.0705707
43. Shigetomi E, Hirayama YJ, Ikenaka K, Tanaka KF, Koizumi S (2018) Role of purinergic receptor P2Y1 in spatiotemporal Ca^{2+} dynamics in astrocytes. J Neurosci 38(6):1383–1395. https://doi.org/10.1523/JNEUROSCI.2625-17.2017
44. Bhattacharya A, Wang Q, Ao H, Shoblock JR, Lord B, Aluisio L, Fraser I, Nepomuceno D, Neff RA, Welty N, Lovenberg TW, Bonaventure P, Wickenden AD, Letavic MA (2013) Pharmacological characterization of a novel centrally permeable P_2X_7 receptor antagonist: JNJ-47965567. Br J Pharmacol 170(3):624–640. https://doi.org/10.1111/bph.12314
45. Kasymov V, Larina O, Castaldo C, Marina N, Patrushev M, Kasparov S, Gourine AV (2013) Differential sensitivity of brainstem versus cortical astrocytes to changes in pH reveals functional regional specialization of astroglia. J Neurosci 33(2):435–441. https://doi.org/10.1523/JNEUROSCI.2813-12.2013
46. Rebola N, Simões AP, Canas PM, Tomé AR, Andrade GM, Barry CE, Agostinho PM, Lynch MA, Cunha RA (2011) Adenosine A_{2A} receptors control neuroinflammation and consequent hippocampal neuronal dysfunction. J Neurochem 117(1):100–111. https://doi.org/10.1111/j.1471-4159.2011.07178.x
47. Kaster MP, Machado NJ, Silva HB, Nunes A, Ardais AP, Santana M, Baqi Y, Müller CE, Rodrigues AL, Porciúncula LO, Chen JF, Tomé ÂR, Agostinho P, Canas PM, Cunha RA (2015) Caffeine acts through neuronal adenosine A_{2A} receptors to prevent mood and memory dysfunction triggered by chronic stress. Proc Natl Sci USA 112(25):7833–7838. https://doi.org/10.1073/pnas.1423088112
48. Silva AC, Lemos C, Gonçalves FQ, Pliássova AV, Machado NJ, Silva HB, Canas PM, Cunha RA, Lopes JP, Agostinho P (2018) Blockade of adenosine A_{2A} receptors recovers early deficits of memory and plasticity in the triple transgenic mouse model of Alzheimer's disease. Neurobiol Dis 117:72–81. https://doi.org/10.1016/j.nbd.2018.05.024
49. Carrasquero LM, Delicado EG, Bustillo D, Gutiérrez-Martín Y, Artalejo AR, Miras-Portugal MT (2009) P2X7 and P2Y13 purinergic receptors mediate intracellular calcium responses to BzATP in rat cerebellar astrocytes. J Neurochem 110(3):879–889. https://doi.org/10.1111/j.1471-4159.2009.06179.x
50. Shinozaki Y, Shibata K, Yoshida K, Shigetomi E, Gachet C, Ikenaka K, Tanaka KF, Koizumi S (2017) Transformation of astrocytes to a neuroprotective phenotype by microglia via $P2Y_1$ receptor downregulation. Cell Rep 19(6):1151–1164. https://doi.org/10.1016/j.celrep.2017.04.047
51. Zhang JM, Wang HK, Ye CQ, Ge W, Chen Y, Jiang ZL, Wu CP, Poo MM, Duan S (2003) ATP released by astrocytes mediates glutamatergic activity-dependent heterosynaptic suppression. Neuron 40(5):971–982. https://doi.org/10.1016/s0896-6273(03)00717-7
52. Kanno T, Nishizaki T (2012) A_{2a} adenosine receptor mediates PKA-dependent glutamate release from synaptic-like vesicles and Ca2+ efflux from an IP)- and ryanodine-insensitive intracellular calcium store in astrocytes. Cell Physiol Biochem 30(6):1398–1412. https://doi.org/10.1159/000343328
53. Fam SR, Gallagher CJ, Kalia LV, Salter MW (2003) Differential frequency dependence of $P2Y_1$- and $P2Y_2$- mediated Ca^{2+} signaling in astrocytes. J Neurosci 23(11):4437–4444. https://doi.org/10.1523/JNEUROSCI.23-11-04437.2003
54. James G, Butt AM (2002) P2Y and P2X purinoceptor mediated Ca2+ signalling in glial cell pathology in the central nervous system. Eur J Pharmacol 447(2–3):247–260. https://doi.org/10.1016/s0014-2999(02)01756-9
55. Svobodova I, Bhattaracharya A, Ivetic M, Bendova Z, Zemkova H (2018) Circadian ATP release in organotypic cultures of the rat suprachiasmatic nucleus is dependent on P2X7 and P2Y receptors. Front Pharmacol 9:192. https://doi.org/10.3389/fphar.2018.00192
56. Salter MW, Hicks JL (1995) ATP causes release of intracellular Ca^{2+} via the phospholipase C beta/IP3 pathway in astrocytes from the dorsal spinal cord. J Neurosci 15(4):2961–2971. https://doi.org/10.1523/JNEUROSCI.15-04-02961.1995
57. Weng JY, Hsu TT, Sun SH (2008) Functional characterization of P2Y1 versus P2X receptors in RBA-2 astrocytes: elucidate the roles of ATP release and protein kinase C. J Cell Biochem 104(2):554–567. https://doi.org/10.1002/jcb.21645
58. Muller MS, Taylor CW (2017) ATP evokes Ca^{2+} signals in cultured foetal human cortical astrocytes entirely through G protein-coupled P2Y receptors. J Neurochem 142(6):876–885. https://doi.org/10.1111/jnc.14119
59. Suadicani SO, Brosnan CF, Scemes E (2006) P_2X_7 receptors mediate ATP release and amplification of astrocytic intercellular Ca^{2+} signaling. J Neurosci 26(5):1378–1385. https://doi.org/10.1523/JNEUROSCI.3902-05.2006
60. D'Alimonte I, Ciccarelli R, Di Iorio P, Nargi E, Buccella S, Giuliani P, Rathbone MP, Jiang S, Caciagli F, Ballerini P (2007) Activation of P2X7 receptors stimulates the expression of P2Y(2) receptor mRNA in astrocytes cultured from rat brain. Int J Immunopathol Pharmacol 20(2):301–316. https://doi.org/10.1177/039463200702000210
61. Dias L, Lopes CR, Gonçalves FQ, Nunes A, Pochmann D, Machado NJ, Tomé AR, Agostinho P, Cunha RA (2021) Crosstalk between ATP-P2X7 and adenosine A2A receptors controlling neuroinflammation in rats subject to repeated restraint stress. Front Cell Neurosci 15:639322. https://doi.org/10.3389/fncel.2021.639322
62. Fredholm BB, Chern Y, Franco R, Sitkovsky M (2007) Aspects of the general biology of adenosine A2A signaling. Prog Neurobiol 83(5):263–276. https://doi.org/10.1016/j.pneurobio.2007.07.005
63. Brodie C, Blumberg PM, Jacobson KA (1998) Activation of the A_{2A} adenosine receptor inhibits nitric oxide production in glial cells. FEBS Lett 429(2):139–142. https://doi.org/10.1016/s0014-5793(98)00556-0

64. Verkhratsky A, Krishtal OA, Burnstock G (2009) Purinoceptors on neuroglia. Mol Neurobiol 39(3):190–208. https://doi.org/10.1007/s12035-009-8063-2
65. Pacholko AG, Wotton CA, Bekar LK (2020) Astrocytes-the ultimate effectors of long-range neuromodulatory networks? Front Cell Neurosci 14:581075. https://doi.org/10.3389/fncel.2020.581075
66. Shigetomi E, Patel S, Khakh BS (2016) Probing the complexities of astrocyte calcium signaling. Trends Cell Biol 26(4):300–312. https://doi.org/10.1016/j.tcb.2016.01.003
67. Bushong EA, Martone ME, Jones YZ, Ellisman MH (2002) Protoplasmic astrocytes in CA1 stratum radiatum occupy separate anatomical domains. J Neurosci 22(1):183–192. https://doi.org/10.1523/JNEUROSCI.22-01-00183.2002
68. Perea G, Araque A (2005) Properties of synaptically evoked astrocyte calcium signal reveal synaptic information processing by astrocytes. J Neurosci 25(9):2192–2203. https://doi.org/10.1523/JNEUROSCI.3965-04.2005
69. Di Castro MA, Chuquet J, Liaudet N, Bhaukaurally K, Santello M, Bouvier D, Tiret P, Volterra A (2011) Local Ca^{2+} detection and modulation of synaptic release by astrocytes. Nat Neurosci 14(10):1276–1284. https://doi.org/10.1038/nn.2929
70. Bonansco C, Couve A, Perea G, Ferradas CÁ, Roncagliolo M, Fuenzalida M (2011) Glutamate released spontaneously from astrocytes sets the threshold for synaptic plasticity. Eur J Neurosci 33(8):1483–1492. https://doi.org/10.1111/j.1460-9568.2011.07631.x
71. Shigetomi E, Saito K, Sano F, Koizumi S (2019) Aberrant calcium signals in reactive astrocytes: a key process in neurological disorders. Int J Mol Sci 20(4):996. https://doi.org/10.3390/ijms20040996
72. Rodrigues RJ, Tomé AR, Cunha RA (2015) ATP as a multi-target danger signal in the brain. Front Neurosci 9:148. https://doi.org/10.3389/fnins.2015.00148
73. Delekate A, Füchtemeier M, Schumacher T, Ulbrich C, Foddis M, Petzold GC (2014) Metabotropic P2Y1 receptor signalling mediates astrocytic hyperactivity in vivo in an Alzheimer's disease mouse model. Nat Commun 5:5422. https://doi.org/10.1038/ncomms6422
74. Reichenbach N, Delekate A, Breithausen B, Keppler K, Poll S, Schulte T, Peter J, Plescher M, Hansen JN, Blank N, Keller A, Fuhrmann M, Henneberger C, Halle A, Petzold GC (2018) P2Y1 receptor blockade normalizes network dysfunction and cognition in an Alzheimer's disease model. J Exp Med 215(6):1649–1663. https://doi.org/10.1084/jem.20171487
75. Chow SK, Yu D, Macdonald CL, Buibas M, Silva GA (2010) Amyloid β-peptide directly induces spontaneous calcium transients, delayed intercellular calcium waves and gliosis in rat cortical astrocytes. ASN Neuro 2(1):e00026. https://doi.org/10.1042/AN20090035
76. Kuchibhotla KV, Lattarulo CR, Hyman BT, Bacskai BJ (2009) Synchronous hyperactivity and intercellular calcium waves in astrocytes in Alzheimer mice. Science 323(5918):1211–1215. https://doi.org/10.1126/science.1169096
77. Lee L, Kosuri P, Arancio O (2014) Picomolar amyloid-β peptides enhance spontaneous astrocyte calcium transients. J Alzheimers Dis 38(1):49–62. https://doi.org/10.3233/JAD-130740
78. Haughey NJ, Mattson MP (2003) Alzheimer's amyloid beta-peptide enhances ATP/gap junction-mediated calcium-wave propagation in astrocytes. Neuromolecular Med 3(3):173–180. https://doi.org/10.1385/NMM:3:3:173
79. Okubo Y (2020) Astrocytic Ca^{2+} signaling mediated by the endoplasmic reticulum in health and disease. J Pharmacol Sci 144(2):83–88. https://doi.org/10.1016/j.jphs.2020.07.006
80. Yu Z, Dou F, Wang Y, Hou L, Chen H (2018) Ca2+-dependent endoplasmic reticulum stress correlation with astrogliosis involves upregulation of KCa3.1 and inhibition of AKT/mTOR signaling. J Neuroinflammation 15(1):316. https://doi.org/10.1186/s12974-018-1351-x
81. Cervetto C, Venturini A, Passalacqua M, Guidolin D, Genedani S, Fuxe K, Borroto-Esquela DO, Cortelli P, Woods A, Maura G, Marcoli M, Agnati LF (2017) A2A–D2 receptor-receptor interaction modulates gliotransmitter release from striatal astrocyte processes. J Neurochem 140(2):268–279. https://doi.org/10.1111/jnc.13885
82. Paiva I, Carvalho K, Santos P, Cellai L, Pavlou MAS, Jain G, Gnad T, Pfeifer A, Vieau D, Fischer A, Buée L, Outeiro TF, Blum D (2019) A2AR-induced transcriptional deregulation in astrocytes: an in vitro study. Glia 67(12):2329–2342. https://doi.org/10.1002/glia.23688
83. Matos M, Shen HY, Augusto E, Wang Y, Wei CJ, Wang YT, Agostinho P, Boison D, Cunha RA, Chen JF (2015) Deletion of adenosine A2A receptors from astrocytes disrupts glutamate homeostasis leading to psychomotor and cognitive impairment: relevance to schizophrenia. Biol Psychiatry 78(11):763–774. https://doi.org/10.1016/j.biopsych.2015.02.026
84. Laurent C, Burnouf S, Ferry B, Batalha VL, Coelho JE, Baqi Y, Malik E, Mariciniak E, Parrot S, Van der Jeugd A, Faivre E, Flaten V, Ledent C, D'Hooge R, Sergeant N, Hamdane M, Humez S, Müller CE, Lopes LV, Buée L, Blum D (2016) A2A adenosine receptor deletion is protective in a mouse model of tauopathy. Mol Psychiatry 21(1):97–107. https://doi.org/10.1038/mp.2014.151
85. Temido-Ferreira M, Ferreira DG, Batalha VL, Marques-Morgado I, Coelho JE, Pereira P, Gomes R, Pinto A, Carvalho S, Canas PM, Cuvelier L, Buée-Scherrer V, Faivre E, Baqi Y, Müller CE, Pimentel J, Schiffmann SN, Buée L, Bader M, Outeiro TF, Blum D, Cunha RA, Marie H, Pousinha PA, Lopes LV (2020) Age-related shift in LTD is dependent on neuronal adenosine A2A receptors interplay with mGluR5 and NMDA receptors. Mol Psychiatry 25(8):1876–1900. https://doi.org/10.1038/s41380-018-0110-9
86. Cunha RA (2016) How does adenosine control neuronal dysfunction and neurodegeneration? J Neurochem 139(6):1019–1055. https://doi.org/10.1111/jnc.13724